CROATICA CHEMICA ACTA
CCACAA **78** (3) 463–477 (2005)

ISSN-0011-1643
*CCA*-3036
*Original Scientific Paper*

# Determination of *Mammillaria gracillis N*-glycan Patterns by ESI Q-TOF Mass Spectrometry*

**Biljana Balen,[a] Alina Zamfir,[b] Sergey Y. Vakhrushev,[b] Marijana Krsnik-Rasol,[a] and Jasna Peter-Katalinić[b,**]**

[a]*Department of Molecular Biology, Faculty of Science, University of Zagreb, Rooseveltov trg 6, HR-10000 Zagreb, Croatia*

[b]*Institute for Medical Physics and Biophysics, University of Muenster, Robert-Koch-Strasse 31, D-48149 Muenster, Germany*

RECEIVED FEBRUARY 11, 2005; REVISED JULY 11, 2005; ACCEPTED JULY 13, 2005

*N*-glycans detached from the 42 kDa cellular glycoprotein of *in vitro* propagated cactus (*Mammillaria gracillis* Pfeiff.) shoots, callus, hyperhydric regenerants and TW tumour were analyzed by mass spectrometry after in-gel deglycosylation of excised protein bands. Mixtures of *N*-glycans were shown by the electrospray MS analysis to be highly complex and heterogeneous. Only a low amount of high-mannose *N*-glycans was present, while the majority of structures were of the complex-type *N*-glycans. A single *N*-glycan structure was observed in the shoot sample, which appeared to be in good correlation with previous results. Similarities of assigned structures were revealed in the callus and tumour tissue while the highest number of different oligosaccharide structures was found in the hyperhydric regenerant. The presence of sialic acid as a constituent of *N*-glycans was indicated by lectin staining, ion exchange chromatography and molecular mapping by mass spectrometry, and could be correlated with the differentiation status of the tissues. Results obtained in this study indicate that different morphological levels can be correlated with the *N*-glycan composition of cellular glycoproteins.

*Keywords*
*Cactaceae*
crown-gall tumour
morphogenesis
*N*-glycans
sialic acid

## INTRODUCTION

Primary protein structure is genetically determined, but by various post-translational modifications of the primary structures proteins modulate their specific biological activities. Glycosylation is one of the most common and important post-translational modifications of proteins. The oligosaccharide chain can be either *N*- or *O*-linked. In endoplasmic reticulum (ER) *N*-glycosylation, a transfer of the lipid-linked precursor oligosaccharide to the asparagine residue of polypeptide synthesized in the rough ER and its attachment via a covalent linkage occurs. This primary oligosaccharide chain structure is further processed during its exit from ER and passage through Golgi apparatus (GA). The latter cell compartment is also a site of protein *O*-glycosylation.

---

* Dedicated to Professor Željko Kućan on the occasion of his 70th birthday. Presented at the Congress of the Croatian Society of Biochemistry and Molecular Biology, $HDBMB_{2004}$, Bjelolasica, Croatia, September 30 – October 2, 2004.

** Author to whom correspondence should be addressed. (E-mail: jkp@uni-muenster.de)

*N*-linked oligosaccharides of plant glycoproteins are covalently linked to the asparagine residues (Asn) within the common consensus polypeptide sequence Asn-Xaa-Ser/Thr (where Xaa is any amino acid other than proline and aspartic acid), as they are in animal glycoproteins, and the core structure, $Man_3$-$GlcNAc_2$-Asn, is also preserved. Oligosaccharide moieties of glycoproteins originating from various organs of different plant species have been investigated. On the basis of these results,[1–3] *N*-glycan classification into four classes has been proposed: i) high-mannose-type, ii) complex-type, iii) paucimannosidic-type and iv) hybrid-type-*N*-glycans. Although the high-mannose type glycan structures of plants are identical to those of animal oligosaccharides, the complex-type, paucimannosidic-type and the hybrid-type glycans characteristically contain $\beta$-xylose linked, $\beta(1\rightarrow2)$, to the core $\beta$-mannose residue. Furthermore, the complex-type glycans often contain $\alpha$-fucose linked, $\alpha(1\rightarrow3)$, to the proximal *N*-acetylglucosamine residue and an $\alpha$-fucose linked, $\alpha(1\rightarrow6)$, to the branching GlcNAc residues. Structures that have not been found in oligosaccharides of plant glycoproteins so far are sialic acids,[1,4,5] $\alpha$-fucose linked, $\alpha(1\rightarrow6)$, to the proximal GlcNAc residue and $\alpha$-fucose linked, $\alpha(1\rightarrow3)$, to the branching GlcNAc residue,[1,5] all of which are typical of animal glycans. In plants, like in other organisms, covalently linked glycans strongly influence the glycoprotein conformation, stability and biological activity. *N*-glycosylated proteins are well known for their antigenic properties. Due to similar glycosylation pathways in plant and animal cells, plant systems have been proposed as a suitable alternative source of therapeutic proteins.[6]

A number of efficient strategies have been developed to study glycoproteins and their attached oligosaccharide structures by mass spectrometry.[7] Of particular relevance are those using proteins separated by 1D- and 2D-PAGE.[8,9] Two modern ionization methods are available for the analysis of proteins and oligosaccharides by mass spectrometry, matrix-assisted laser desorption ionization (MALDI) and electrospray ionization (ESI). MALDI has proved to be very efficient for analyses of plant glycoproteins[3,10,11] and it is often used for determination of the structure and distribution of plant *N*-glycans on a protein backbone. ESI was less frequently used for analyses of oligosaccharide mixtures of plant origin although it has been successfully applied for determination of the structure and distribution of *N*-glycans of S-RNAses of *Nicotiana alata*[11]and the analysis of *N*-glycans of seven S-RNAses in *Pyrus pyrifolia*.[12]

It has been postulated that the morphogenic events are followed by a change in protein *N*-glycosylation.[11,14] Analysis of these changes should allow estimation of post-translational modification specificity in a certain developmental stage. Relatively little is known about the effects of the environmental conditions and developmental stage on proteins produced by plant tissues cultured *in vitro*. Artificial environmental conditions in tissue culture, such as high relative humidity and rich nutrient medium, can alter tissue growth.[15] *Mammillaria gracillis* shoots, propagated *in vitro*, were shown to develop callus even in the absence of exogenous growth regulators. This habituated callus regenerates morphologically normal and hyperhydric shoots. *Mammillaria* was susceptible to tumour transformation by the *Agrobacteria*-Ti-plasmid-system.[16]

In the present study, the composition of *N*-glycans released in-gel from the selected cellular glycoprotein (42 kDa) of the shoot, callus, hyperhydric regenerants and TW tumour was comparatively analyzed by ESI-Q-TOF mass spectrometry.

## EXPERIMENTAL

### *Reagents and Materials*

Methanol, acetonitrile and sodium bicarbonate were obtained from Merck (Darmstadt, Germany) and used without further purification. Distilled and deionized water from Mili-Q water systems (Millipore, Bedford, MA, USA) was used for preparation of the sodium bicarbonate buffer and for sample solutions. Aqueous sample solutions were dried in a Speed-Vac SPD 111V evaporator (Savant, Düsseldorf, Germany). The pH value of the sodium bicarbonate buffer was adjusted by a 766 pH-meter Calimatic (Knick, Germany).

### *Plant Material*

The following plant material was used in the study: cactus *Mammillaria gracillis* Pfeiff. shoots, callus, regenerants (normal and hyperhydric) and TW tumour. All tissues were cultivated *in vitro*, on solid, hormone-free MS nutrient medium (0.9 % agar, 3 % sucrose)[17] under 16/8-hour-light/night-photoperiod (light intensity 90 $\mu E\ s^{-1}\ m^{-2}$) at 24 °C. Under the culture conditions, approximately 100 % of cactus plants produced abundant callus.[16] This callus was subcultivated on the same hormone-free medium, expressed a high morphogenic capacity, regenerating phenotypically normal and malformed hyperhydric shoots. Tumour tissue culture was established from primary tumours induced on shoot explants by *Agrobacterium tumefaciens,* the wild strain B6S3 (tumour line TW).[16] Transformed tissues never expressed any morphogenic capacity.

### *Protein Samples and SDS-PAGE*

Tissue samples were frozen at –80 °C and lyophilized before protein extraction. Total soluble proteins were extracted by grinding 0.5 g of tissue in 1.5 ml of 0.1 M Tris-HCl buffer, pH = 8.0, at 4 °C. Homogenates were centrifuged at 20 000 *g* and 4 °C for 15 min. Supernatants were centrifuged again at 20 000 *g* and 4 °C for 60 min. Protein content was determined according to Bradford.[18] Samples were denaturated using 0.125 M Tris buffer (pH = 6.8), containing

5 % $\beta$-mercaptoethanol and 2 g/100 ml SDS (sodium dodecyl sulphate). For the SDS-PAGE, the same amount of protein (5–8 μg) per sample was loaded. Cellular proteins were analyzed by SDS electrophoresis in 10 % T (2.67 % C) polyacrylamide gels, with the buffer system of Laemmli.[19] Protein bands were visualized by 0.1 % Coomassie blue R-250 or silver stained.[20]

### *Electroblotting and Lectin Staining*

Proteins from gels were transferred to a nitrocellulose membrane (Pure nitrocellulose membrane – 0.45 μm, Bio-Rad) with a mini trans blot cell (Bio-Rad) in 20 mmol $dm^{-3}$ Tris-HCl, 150 mmol $dm^{-3}$ glycine and 10 % methanol at 60 V for 60 min. The glycan part of *Mammillaria* glycoproteins of 42 kDa was characterized according to the binding of biotin- (Sigma) and/or digoxigenin-labelled lectins (DIG Glycan Differentiation Kit, Roche Diagnostics) specific for binding to sialylated glycoproteins: MAA (lectin from *Maackia amurensis*), specific to sialic acid-(2→3)-α-galactose and SNA (lectin from *Sambucus nigra*), specific to sialic acid-(2→6)-α-galactose. Biotin-labelled lectins were used at a concentration of 20 μl/ml (MAA) and 5 μl/ml (SNA). Detection procedures included the use of interaction between biotin and streptavidin conjugated to alkaline phosphatase. NBT/BCIP solution was used for visualization of the bands. Tested digoxigenin-labelled lectins were used at a concentration of 1 μl /ml (SNA) and 5 μl /ml (MAA). The staining procedure was performed following the manufacturer's instructions.

### *Building Block Analysis by HPAEC*

Oligosaccharide samples of all *Mammillaria* tissues released from 42 kDa glycoprotein with PNGase F were submitted to mild acid hydrolysis (1 M HCl, 80 °C for 60 min). Obtained monosaccharides were separated by high-performance anion exchange chromatography (HPAEC) on a CarboPac™ PA-1 chromatography column (Dionex). The running conditions were: 100 mmol $dm^{-3}$ NaOH/50 mmol $dm^{-3}$ NaOAc gradient to 100 mmol $dm^{-3}$ NaOH/180 mmol $dm^{-3}$ NaOAc at a flow rate of 1 ml/min. Commercially available Neu5Ac (*N*-acetylneuraminic acid) and Neu5Gc (*N*-glycolylneuraminic acid) were used as standard sialic acids.

### *In-gel Deglycosylation with PNGase F*

The basic procedure for in-gel deglycosylation[21] was applied. The 42 kDa bands of shoot, callus, hyperhydric regenerant and TW tumour were excised with a scalpel from Coomassie brilliant blue stained gels and were subjected to in-gel deglycosylation.[22] Bands were first destained with a water solution of 30 % methanol and 7.5 % acetic acid. Even if gel pieces were incompletely destained, no adverse effect on the subsequent *in situ* deglycosylation was observed. Excised gel pieces were washed two times for 30 minutes in 20 mol $dm^{-3}$ $NaHCO_3$, pH = 7.2. The washing liquid was removed and replaced by 900 ml of fresh 20 mmol $dm^{-3}$ $NaHCO_3$, pH = 7.2. To this solution, 60 μl of 45 mmol $dm^{-3}$ DTT was added and the protein was reduced for 30 min at 60 °C. The DTT solution was allowed to cool and 60 μl of 100 mmol $dm^{-3}$ iodoacteamide was added and the protein was alkylated for 30 min in the dark, at room temperature. The solution was removed and the gel pieces were washed two times for 30 minutes in the mixture of acetonitrile and 20 mmol $dm^{-3}$ $NaHCO_3$, (vol. ratio 1:1) pH = 7.2. This solution was removed and the gel pieces were completely dried in SpeedVac.

To the dried gel pieces, 30 μl of the PNGase F solution (100 units/500 μl) (Roche, Mannheim, Germany) was added and incubated for 60 min at 37 °C. Gel pieces were covered with additional 20 mmol $dm^{-3}$ $NaHCO_3$, pH = 7.2, and incubated overnight at 37 °C. Glycans were extracted from the gel pieces by removing the incubation buffer, followed by two extractions with approx. 200 ml of pure water and two extractions with 50 % acetonitrile with sonification for 30 min each. All extracts were combined and dried in vacuum.

*N*-glycans obtained by in-gel deglycosylation were purified using graphitized carbon columns following the described procedure.[22,23] Prior to use, the columns were washed with three changes of 50 μl 80 % acetonitrile in 0.1 % aqueous TFA followed by 3 × 50 μl of water. After that, the samples were applied to the columns. Salts were then washed off with 3 × 50 μl water. *N*-glycans were eluted by 3 × 50 μl of 80 % acetonitrile in 0.1 % aq. TFA, fractions were collected and dried in vacuum. Fractions were dissolved in methanol for MS analysis.

### *ESI-Q-TOF Mass Spectrometry*

Mass spectrometry was performed on an orthogonal hybrid quadrupole time-of-flight mass spectrometer (QTOF™ Micromass, Manchester, U.K.) equipped with a nanoelectrospray ion source in Micromass Z-spray configuration. The QTOF mass spectrometer was interfaced with a PC computer running the MassLynx N.T. software system to control the instrument, acquire and process MS data. The first set of experiments was conducted in the positive ion mode using capillary-based nanoelectrospray for sample infusion into MS. In these experiments, the sample solution was introduced into omega glass capillaries purchased from Hilgenberg, Germany, and in-house pulled using a vertical pipette puller model 720 (David Kopf Instruments, Tujunga, CA, USA). ESI voltage was applied to the solution via a stainless steel wire inserted into the capillary. The spray was initiated at 1.0 kV applied to the nanosprayer and 40–50 V counterelectrode (cone) potential.

For the second set of experiments, fully automated chip-based nanoelectrospray (FACESI) in the negative ion mode was employed for automatic infusion of the sample into MS via chip ionization. FACESI was performed on a NanoMate®100 robot incorporating ESI Chip™ technology (Advion BioSciences, Ithaca, USA) mounted to the QTOF mass spectrometer. The robot was controlled and manipulated by the ChipSoft™ software operating under Windows$^{XP}$. The position of the electrospray chip was adjusted with respect to the cone to ensure optimal transfer of the ionic species into the mass spectrometer. To prevent contamination, a

glass coated microtitre plate was used for all experiments. 2–5 µl aliquots of the working sample solutions were loaded onto a 96-well plate. Following the procedure previously described[24] the robot was programmed to aspirate the sample, followed by 2 µl of air into the pipette tip, and to deliver the sample to the inlet side of the microchip. Electrospray was initiated by applying voltages between 1.45 kV to 1.8 kV and a head pressure of 0.3 to 0.9 p.s.i. After the sample infusion and MS analysis, the ESI pipette tip was ejected and a new tip and chip nozzle were used for each sample. For all experiments desolvation was effective at a source-block temperature of 80 °C and 50 L/h nitrogen flow-rate. All mass spectra were externally calibrated using sodium iodide as a reference.

## RESULTS

### *CBB Protein Pattern*

Glycoprotein of 42 kDa was present in all cactus tissues, on Coomassie brilliant blue stained gels and it was excised for in gel-deglycosylation (Figure 1).

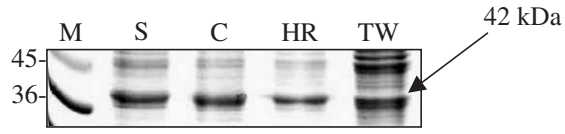


Figure 1. Soluble cellular proteins of *Mammillaria gracillis* tissues separated by 1-D SDS-PAGE and stained with Coomassie brilliant blue. M – molecular mass marker, S – shoot, C – callus; HR – hyperhydric regenerant, TW – TW tumour. The arrow indicates the position of excised 42 kDa glycoprotein.

### *SNA- and MAA-binding Patterns*

Both lectins, which specifically bind to syalilated glycoproteins, gave positive results with glycoproteins of different *Mammillaria gracillis* tissues. The biotin-labelled-SNA-binding pattern showed a very intensive band of 92 kDa in all cactus tissues; the 42 kDa glycoprotein was also present in all examined tissues, although the staining intensity was weaker. Treatment of the membrane with the digoxigenin-labelled-SNA gave a very similar pattern; however, it revealed the presence of an additional band of 44 kDa in the callus, hyperhydric regenerant and TW tumour (Figure 2a).

When glycoproteins were probed with the biotin-labelled-MAA, the very intense 92 kDa band was again detected in all tissues. The 42 and 44 kDa glycoproteins were visible as faint bands in all samples, while the 30 kDa one was present only in the callus, hyperhydric regenerant and TW tumour (Figure 2c). The digoxigenin-labelled-MAA-binding pattern revealed the presence of the 92 kDa band only in the TW tumour, while the 42 and 44 kDa glycoproteins were still present in all cactus

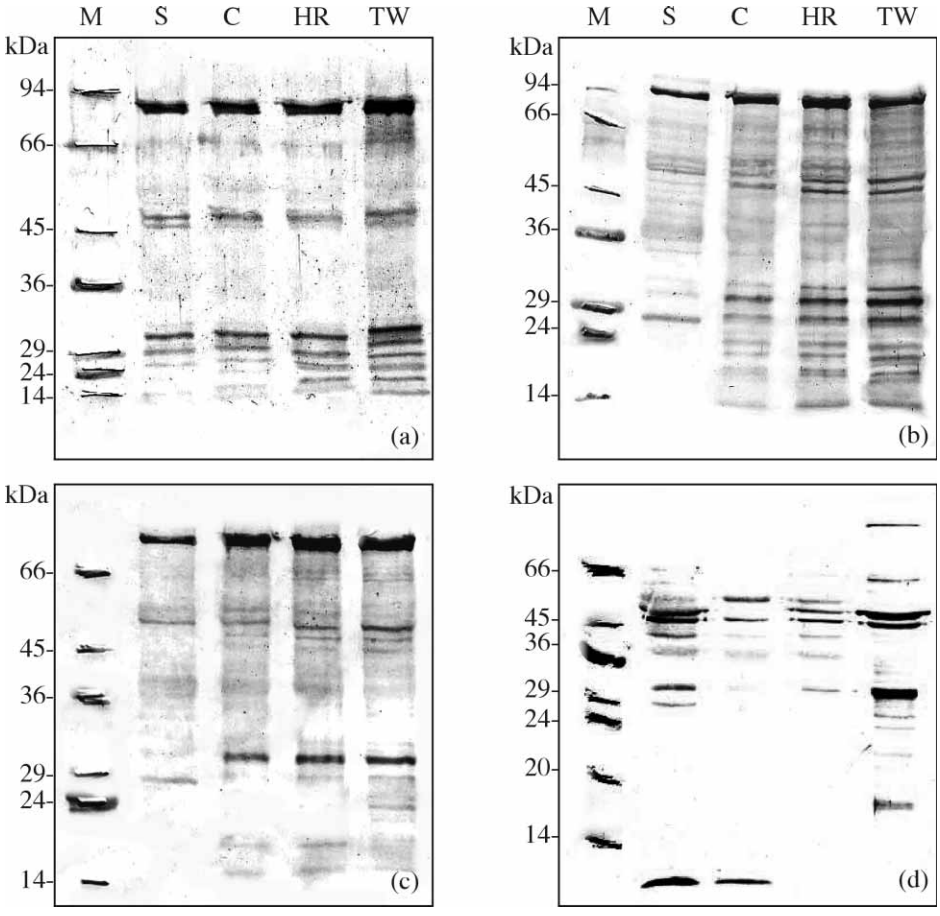


Figure 2. Glycoprotein pattern of different *Mammillaria* tissues according to lectin binding: (a) SNA-biotin-labelled; (b) SNA-digoxigenin-labelled; (c) MAA-biotin labelled; (d) MAA-digoxigenin-labelled after SDS-PAGE and transfer to the nitrocellulose membrane. M – molecular mass markers, S – cactus shoot, C – habituated callus; HR – hyperhydric regenerant, TW – tumour TW.

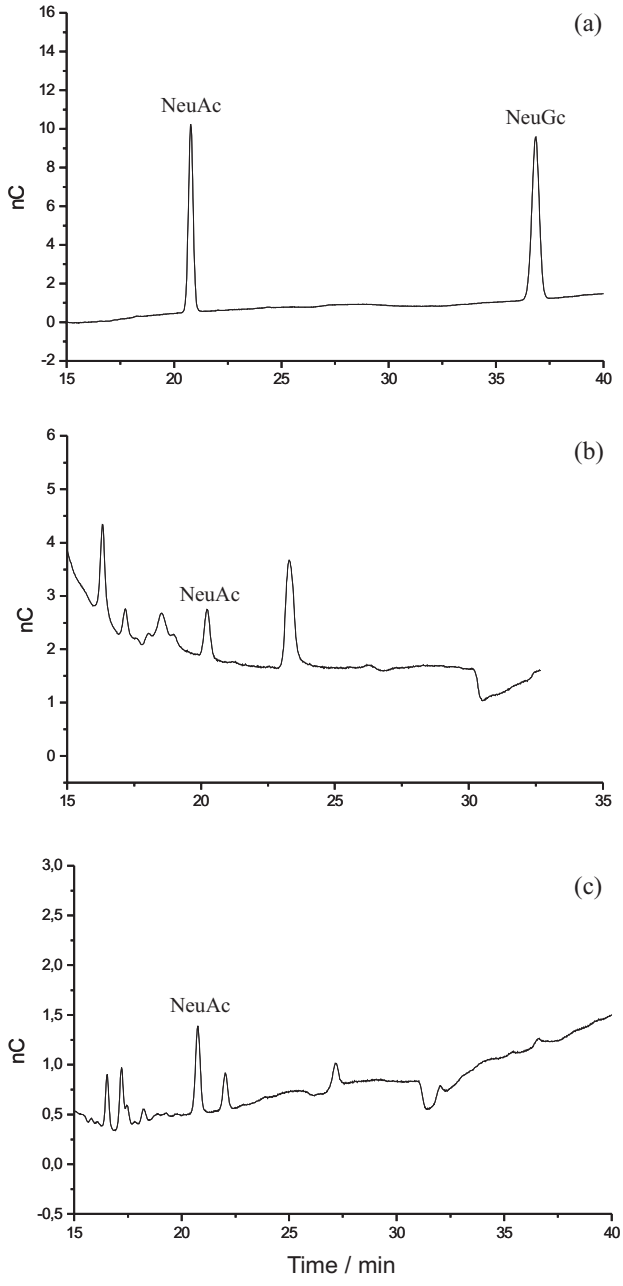


**Figure 3.** HPAEC-PAD profiles of (a) a mixture of commercially available Neu5Ac and Neu5Gc monosaccharides, (b) the total hydrolysate of the hyperhydric regenerant (HR) *N*-glycan fraction, and (c) the total hydrolysate of the tumour tissue (TW) *N*-glycan fraction.

tissues. The 30 kDa band was visible in all tissues, although the staining activity was the strongest in tumour tissue (Figure 2d).

### *Total Hydrolysis Results*

Analysis of totally hydrolyzed samples on anion-exchange chromatography showed the presence of Neu5Ac in both HR and TW glycans, released from the 42 kDa glycoprotein, while Neu5Gc could not be detected (Figure 3).

### *Composition of a Shoot* N-*glycan*

In the negative chip nanoESI MS of shoot glycans, a single truncated paucimannosidic type *N*-glycan, $Hex_2dHex_1HexNAc_2$, could be detected as a singly charged molecular $[M-H]^-$ ion at *m/z* 892.86 (data not shown).

### *Composition of Callus* N-*glycans*

Callus oligosaccharide sample obtained after in-gel deglycosylation of the 42 kDa glycoprotein band was shown by the negative chip-based nanoESI MS to contain a series of high-mannose type *N*-glycans ($Hex_4HexNAc_2$ – $Hex_7HexNAc_2$). Singly charged ions, generated as chloride adducts, were at *m/z* 1107.12 (Figure 4b), *m/z* 1269.10 (Figure 4c), *m/z* 1431.08 and at *m/z* 1593.01 (Figure 4d). Oligosaccharide structures $Hex_6HexNAc_2$ and $Hex_7HexNAc_2$ were detected as doubly charged ions generated as adducts of two chlorides at *m/z* 733.18 and at *m/z* 814.17 (Figure 4a). All structural assignments are summarized in Table I.

A paucimannosidic type *N*-glycan with one pentose residue, $Hex_3HexNAc_2Pent_1$, was detected at *m/z* 1065.19 as a singly charged anion, containing one sodium adduct as well as at *m/z* 1077.27 as a singly charged ion with one chlorine adduct (Figure 4b). The paucimannosidic oligosaccharide containing both fucose and pentose, $Hex_2dHex_1HexNAc_2Pent_1$, was detected as a singly charged ion at *m/z* 1025.16 and as a singly charged ion with one sodium adduct at *m/z* 1049.02 (Figure 4b). A similar structure with two pentose molecules, $Hex_2dHex_1HexNAc_2Pent_2$, was observed at *m/z* 1180.66 (Figure 4c). In the nanoESI QTOF mass spectrum of the callus, two complex type *N*-glycans containing fucose as well as pentose ($Hex_4dHex_1HexNAc_2Pent_1$ and $Hex_5dHex_1HexNAc_2Pent_1$) were detected as singly charged ions at *m/z* 1349.04 (Figure 4c) and *m/z* 1512.08 (Figure 4d).

### *Composition of HR* N-*glycans*

Most of the HR *N*-glycan structures detected in the positive ion mode ESI mass spectrum could represent complex type structures according to the calculations and correlation with known structures published by other authors and present in the data base *N*-glycans SweetDB, German Cancer Research Center Heidelberg, Germany.[25] According to the proposed or postulated biosynthetic routes for glycosylation of plant proteins,[26,27] a number of unusual structures could be derived from the *m/z* values of molecular ions detected by positive nanoESI MS, as summarized in Table II. The values were calculated either as singly protonated, singly sodiated or doubly sodiated molecular ion adducts. The adduct at *m/z* 1106.16 ($Hex_2HexNAc_3Pent_1$) could be considered as a singly charged sodium adduct and the one at *m/z* 1249.16 ($Hex_4HexNAc_2Pent_1$) as a singly charged ion containing two sodium ions, one exchanged for a proton (Figures 5a and

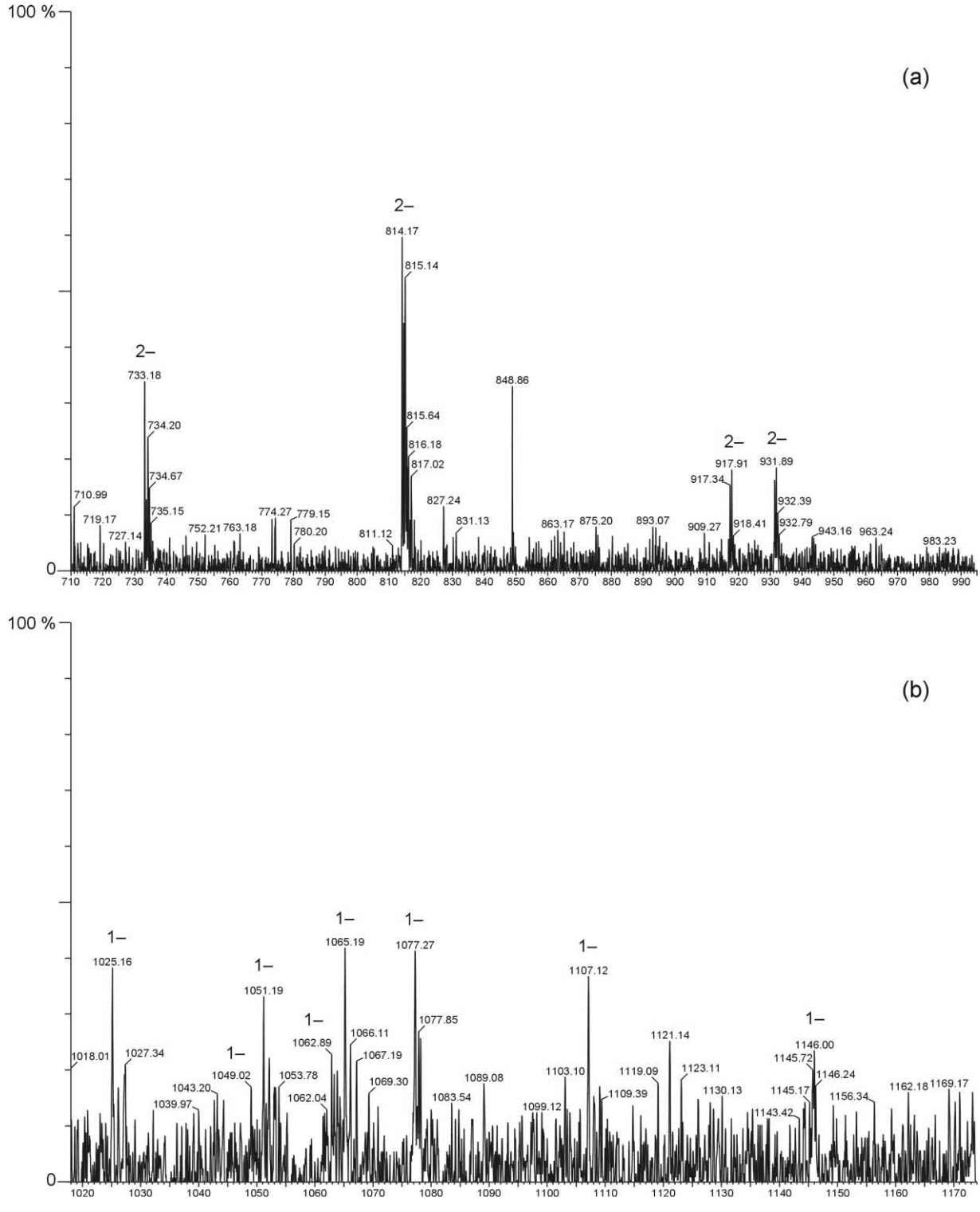


Figure 4., cont. ⇒

5b). Four singly charged ions were considered as singly or doubly sodiated species at *m/z* 1242.06 ($Hex_4dHex_1HexNAc_2$), at *m/z* 1612.03, ($Hex_4dHex_2HexNAc_3$), at *m/z* 1607.07, at *m/z* 1628.03 as ($Hex_5dHex_1HexNAc_3$) while at *m/z* 2111.93 ($Hex_7dHex_1HexNAc_4$) they could be probably fucosylated according to this calculation (Figure 5). Complex-type *N*-glycans, which do not contain pentose or fucose residues, were detected as singly charged ions at *m/z* 1055.38 and at *m/z* 1090.21 ($Hex_4HexNAc_2$, Figure 5a), at *m/z* 2088.90 ($Hex_4HexNAc_7$, Figure 5d) as well as at *m/z* 2538.64 as an ion with two sodium adducts ($Hex_4HexNAc_9$, Figure 5e).

Hypothetically, some of the observed structures could be assigned to oligosaccharides containing sialic acid: two

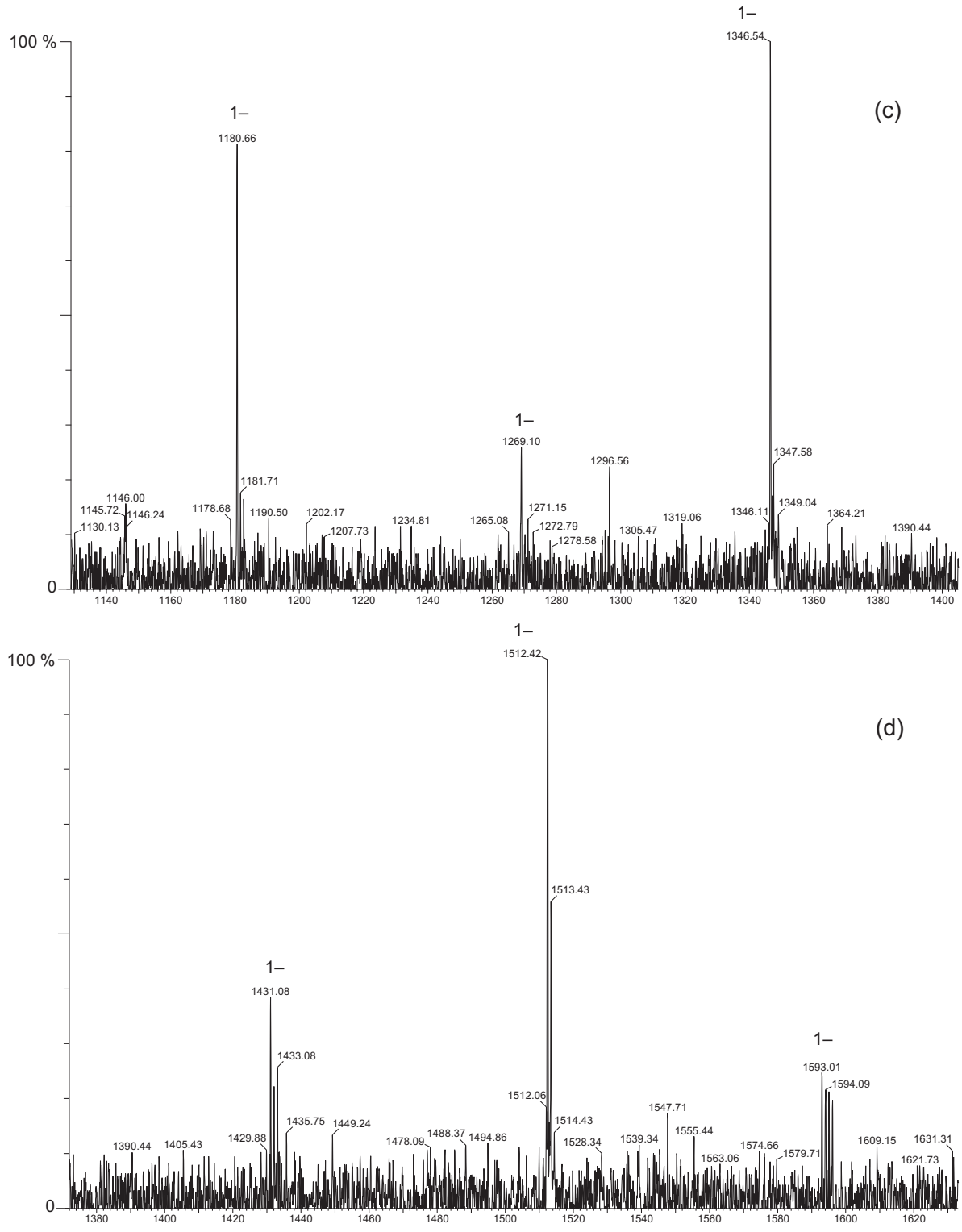


Figure 4. Negative chip-based nanoESI-QTOF MS spectrum of the callus *N*-glycans released with PNGase F from the 42 kDa glycoprotein excised from Coomassie stained gel: assigned structures in the mass range of *m/z* 710–990 (a), *m/z* 1020–1170 (b), *m/z* 1140–1400 (c) and *m/z* 1380–1620 (d).

structures detected as singly charged ions at *m/z* 2036.80 ($Hex_6dHex_1HexNAc_3NeuAc_1$ of theoretical *m/z* value 2036.71) and at *m/z* 2138.65 as an ion with two sodium adducts ($Hex_6HexNAc_4NeuAc_1$ of theoretical *m/z* value 2093.74) could contain one sialic acid moiety according to calculations. Three oligosaccharides could contain two sialic acid moieties: those detected at *m/z* 2061.88 and at *m/z* 2083.95 can be correlated to $Hex_4HexNAc_4NeuAc_2$, that at *m/z* 2429.76 to $Hex_6HexNAc_4NeuAc_2$ and that at *m/z* 2588.91 to $Hex_6HexNAc_5NeuAc_2$. The ions at *m/z*

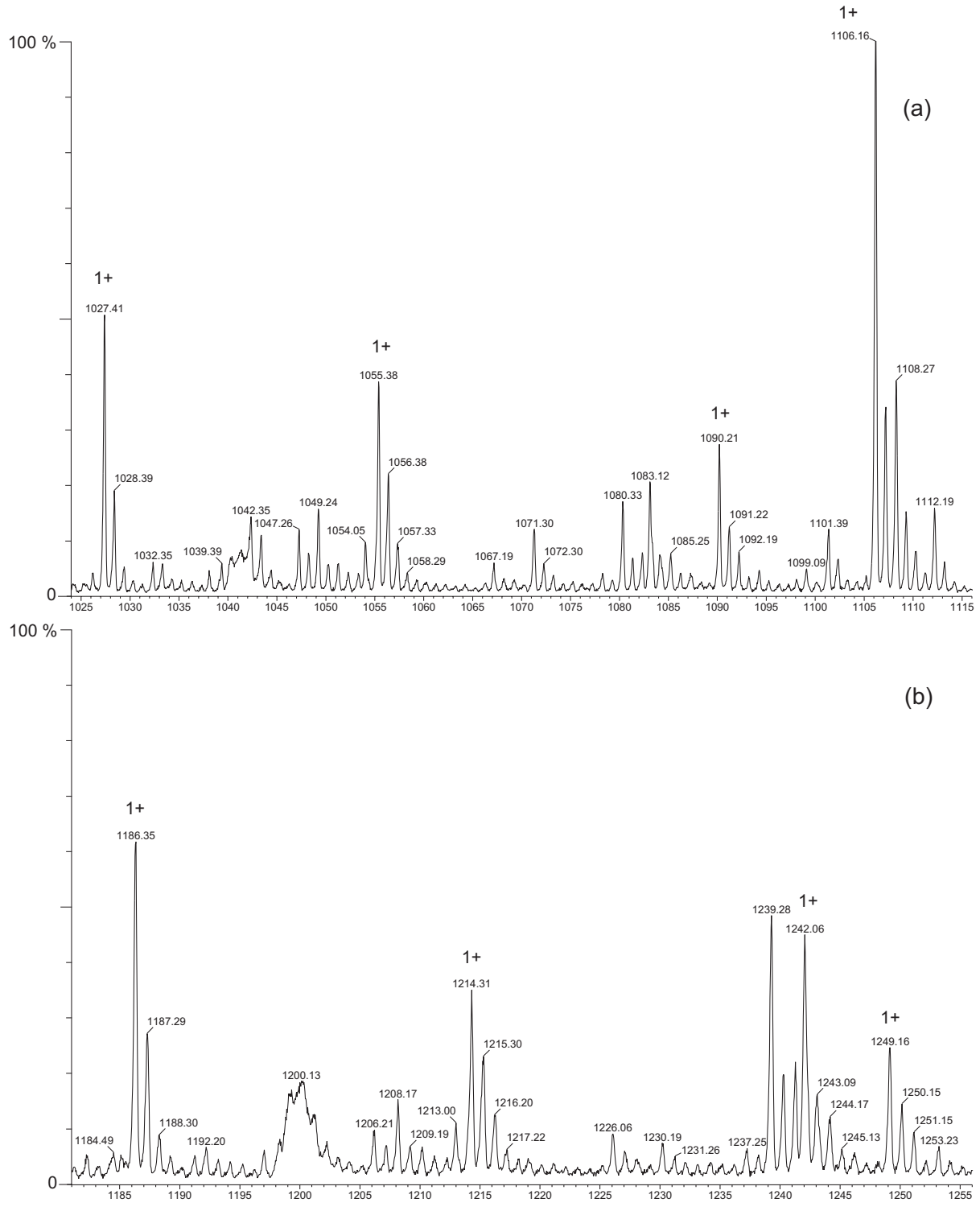


Figure 5., cont. ⇒

2515.69 ($Hex_5HexNAc_4NeuAc_3$) could contain three sialic acid moieties according to these calculations (Figure 5).

Oligosaccharides from 42 kDa glycoprotein from HR delivered in the positive ion mode nanoESI MS a singly charged ion at *m/z* 1027.41, which could be assigned to the paucimannosidic oligosaccharide structure ($Hex_2dHex_1$-$HexNAc_2Pent_1$) (Figure 5a), and the one at *m/z* 2532.71 calculated for assignment to an unusual high-mannose type *N*-glycan ($Hex_{13}HexNAc_2$) (Figure 5e).

### *Composition of TW* N-*glycans*

Figure 6 shows the negative chip-based nanoESI-QTOF MS spectrum of the TW tumour *N*-glycans. Molecular ion species depicted in Figure 4 are presented in Table

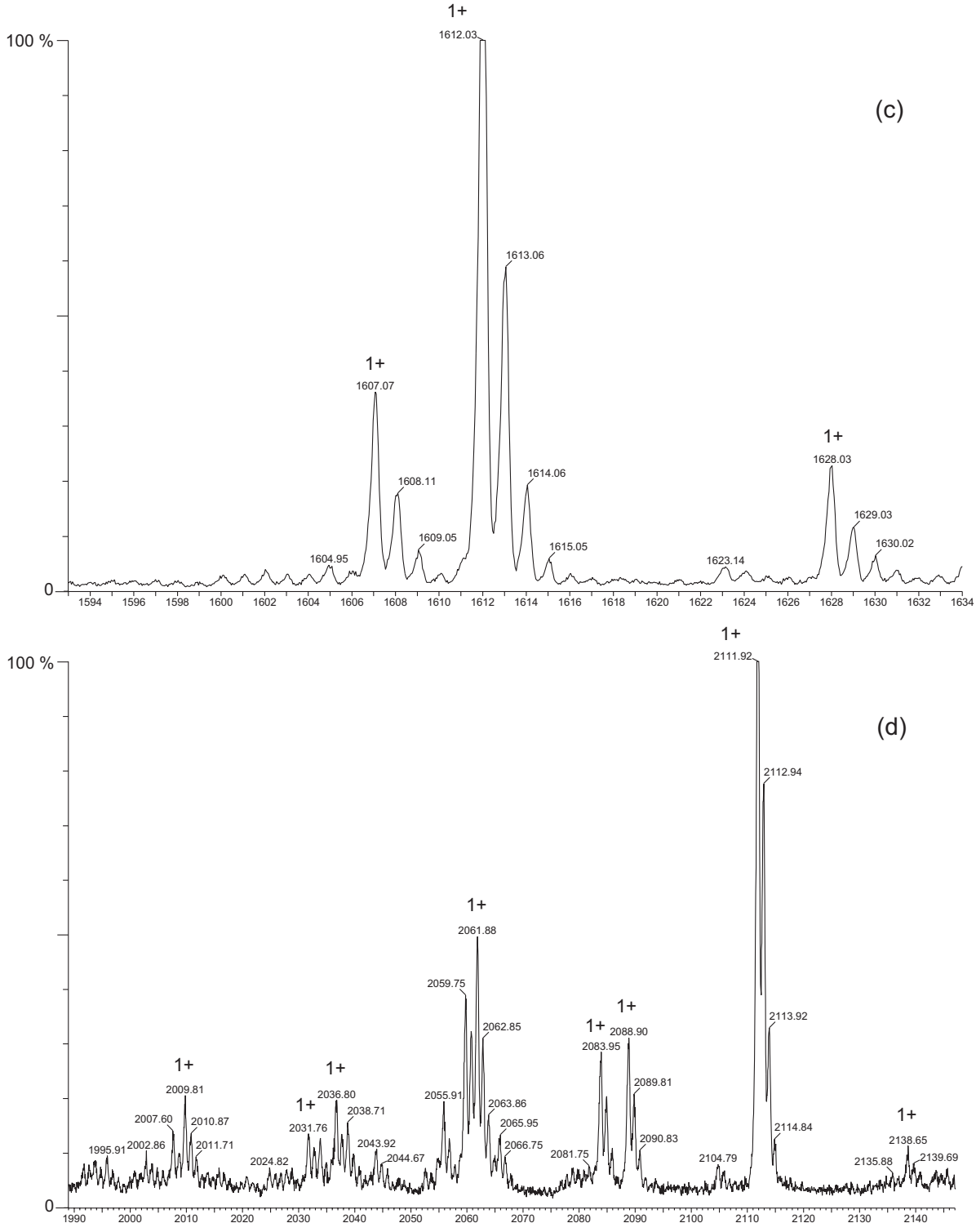


Figure 5., cont. ⇒

III along with the proposed assignment of the *N*-glycans composition and the calculated theoretical values of their corresponding *m/z* values. A series of high-mannose type *N*-glycans ($Hex_3HexNAc_2$ – $Hex_7HexNAc_2$) were detected as singly charged ions generated as chloride adducts at *m/z* 945.23, *m/z* 1107.24 (Figure 6a), at *m/z* 1269.28, *m/z* 1431.308 and at *m/z* 1593.33, respectively (Figure 6b). Oligosaccharide species $Hex_6HexNAc_2$ and $Hex_7HexNAc_2$ were present as doubly charged two chlorides adducts at *m/z* 733.15 and at *m/z* 814.14 (Figure 6a).

A series of dehydrated complex-type *N*-glycans calculated to contain one pentose residue ($Hex_4HexNAc_2Pent_1$ – $Hex_7HexNAc_2Pent_1$) were detected as singly charged ions at *m/z* 1185.26 (Figure 6a), at *m/z* 1347.30,

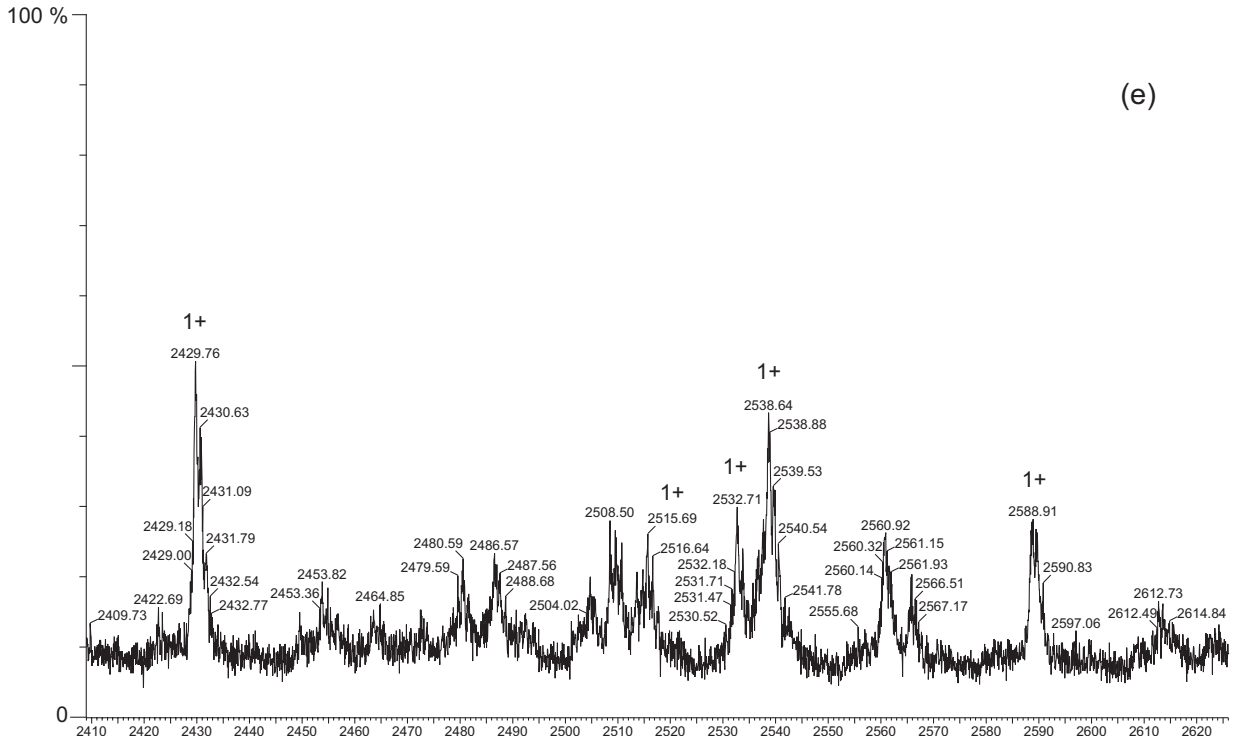


Figure 5. Positive nanoESI-QTOF spectrum of the hyperhydric regenerant *N*-glycans released with PNGase F from the 42 kDa glycoprotein excised from Coomassie stained gel: assigned structures in the mass range of *m/z* 1025–1115 (a), *m/z* 1180–1255 (b), *m/z* 1594–1634 (c), *m/z* 1990–2140 (d) and *m/z* 2410–2620 (e).

*m/z* 1509.33 and at *m/z* 1671.37 (Figure 6b), while the oligosaccharide observed as a singly charged ion at *m/z* 1155.24 (Figure 6a) could contain two pentose moieties ($Hex_3HexNAc_2Pent_2$). Two previously mentioned complex-type structures, $Hex_3HexNAc_2Pent_1$ and $Hex_4HexNAc_2Pent_1$, were also detected as singly charged chloride adducts at *m/z* 1077.24 and at *m/z* 1239.28, respectively (Figure 6a).

TABLE I. Assignment of *N*-glycan molecular ions detected by negative chip-based nanoESI-QTOF MS after in-gel release from the 42 kDa callus glycoprotein with PNGase F

| $[M+2Cl]^{2-}$ | $[M+Cl-H]^{2-}$ | $[M+Cl]^-$ | $[M+Na-2H]^-$ | $[M-H]^-$ | Theoretical mass | Proposed structure | *N*-glycan type |
|---|---|---|---|---|---|---|---|
| | 917.34 | | | | 1802.63 | $Hex_6HexNAc_4$ | complex |
| | 931.39 | | | | | n.a. | |
| | 1347.71 | | | | 2661.95 | $Hex_7HexNAc_6NeuAc_1$ | complex |
| | | 1107.12 | | | 1072.38 | $Hex_4HexNAc_2$ | high-mannose |
| | | 1269.10 | | | 1234.35 | $Hex_5HexNAc_2$ | high-mannose |
| 733.18 | | 1431.08 | | | 1396.49 | $Hex_6HexNAc_2$ | high-mannose |
| 814.17 | | 1593.01 | | | 1558.54 | $Hex_7HexNAc_2$ | high-mannose |
| | | 1077.27 | 1065.19 | | 1042.38 | $Hex_3HexNAc_2Pent_1$ | paucimannosidic |
| | | | 1049.02 | 1025.16 | 1026.38 | $Hex_2dHex_1HexNAc_2Pent_1$ | paucimannosidic |
| | | | 1180.66 | | 1158.43 | $Hex_2dHex_1HexNAc_2Pent_2$ | complex |
| | | | | 1349.04 | 1350.40 | $Hex_4dHex_1HexNAc_2Pent_1$ | complex |
| | | | | 1512.08 | 1512.53 | $Hex_5dHex_1HexNAc_2Pent_1$ | complex |
| | | 1051.19 | | | | n.a. | |
| | | | | 1146.00 | | n.a. | |

TABLE II. Assignment of *N*-glycan molecular ions detected by positive ion nanoESI-QTOF MS after in-gel release from the 42 kDa hyperhydric regenerant glycoprotein with PNGase F

| $[M+2Na-1H]^+$ | $[M+Na]^+$ | $[M+H]^+$ | Theoretical mass | Proposed structure | *N*-glycan type |
|---|---|---|---|---|---|
| | | 1027.41 | 1026.38 | $Hex_2dHex_1HexNAc_2Pent_1$ | paucimannosidic |
| | | 1055.38 | | $Hex_4HexNAc_2$-$H_20$ | complex |
| | | 1090.21 | | $Hex_4HexNAc_2$+$H_20$ | complex |
| | 1106.16 | | 1083.41 | $Hex_2HexNAc_3Pent_1$ | complex |
| | | 1186.35 | 1185.43 | | |
| | | 1214.31 | | n.a. | |
| | 1242.06 | | 1218.44 | $Hex_4dHex_1HexNAc_2$ | complex |
| 1249.16 | | | 1204.43 | $Hex_4HexNAc_2Pent_1$ | complex |
| 1612.03 | | | 1567.57 | $Hex_4dHex_2HexNAc_3$ | complex |
| 1628.03 | 1607.07 | | 1583.37 | $Hex_5dHex_1HexNAc_3$ | complex |
| 2009.81 | | | 1964.69 | $Hex_7HexNAc_4$ | complex |
| | | 2031.76 | 2030.75 | $Hex_4dHex_1HexNAc_6$ | complex |
| | | 2036.80 | 2036.71 | $Hex_6dHex_1HexNAc_3NeuAc_1$ | complex |
| | 2083.95 | 2061.88 | 2060.73 | $Hex_4HexNAc_4NeuAc_2$ | complex |
| | | 2088.90 | 2087.77 | $Hex_4HexNAc_7$ | complex |
| | | 2111.93 | 2110.76 | $Hex_7dHex_1HexNAc_4$ | complex |
| 2138.65 | | | 2093.74 | $Hex_6HexNAc_4NeuAc_1$ | complex |
| 2429.76 | | | 2384.84 | $Hex_6HexNAc_4NeuAc_2$ | complex |
| | | 2515.69 | 2513.88 | $Hex_5HexNAc_4NeuAc_3$ | complex |
| | | 2532.71 | 2530.85 | $Hex_{13}HexNAc_2$ | high-mannose |
| 2538.64 | | | 2493.93 | $Hex_4HexNAc_9$ | complex |
| | | 2588.91 | 2587.92 | $Hex_6HexNAc_5NeuAc_2$ | complex |

The second series of dehydrated complex oligosaccharides should contain one pentose and one deoxyhexose (fucose) residue ($Hex_2dHex_1HexNAc_2Pent_1$ – $Hex_5dHex_1HexNAc_2Pent_1$), as detected by singly charged ions at *m/z* 1007.18, at *m/z* 1139.22 (Figure 6a), at *m/z* 1331.29 and at *m/z* 1493.33, respectively (Figure 6b).

Composition of the fucosylated paucimannosidic type *N*-glycan, $Hex_2dHex_1HexNAc_2$, detected as a singly charged ion at *m/z* 893.02 (Figure 6a), could be correlated to the series of paucimannosidic oligosaccharides containing both pentose and deoxyhexose (fucose), such as $Hex_1dHex_1HexNAc_2Pent_1$ – $Hex_3dHex_1HexNAc_2Pent_1$, observed as singly charged ions at *m/z* 863.18, at *m/z* 1025.22 and at *m/z* 1187.25, respectively (Figure 6a).

## DISCUSSION

Proteins as direct gene products reflect characteristic gene expression from different tissues and changes in the protein pattern that could possibly be correlated to different levels of development and differentiation. The glycosylation profile of endogenous proteins can be modulated by plant development and growth conditions.[10] The analysis of *N*-linked glycans of soluble endogenous glycoproteins from the leaves of tobacco plants of different age and under different conditions demonstrated that developmental processes in plants could influence glycosylation.[11] In our study, the 42 kDa protein band was previously detected by 1-D electrophoresis in all cactus tissues, while the corresponding glycoprotein of 42 kDa, reacting with Con A, was highly expressed only in the callus, hyperhydric regenerants and in tumour extracts but not in shoots.[28] These results suggested that the 42 kDa protein, although present in all investigated tissues, expresses in different tissues different sugar composition, where glycosylation might be missing in the cactus shoot. In order to establish primary glycosylation patterns, glycans were released from the parent glycoprotein by in-gel deglycosylation reaction and were submitted to identification by mass spectrometry for molecular mapping. ESI-Q-TOF MS analysis of *N*-glycans released with PNGase F from the 42 kDa glycoprotein revealed that mixtures of oligosaccharides released from the callus, hyperhydric regenerant and TW tumour are complex and highly heterogeneous. In all these samples, a certain low amount of high-Man *N*-glycans was detected. Most of the structures could be assigned by calculation to complex-type *N*-glycans, expected to contain either Xyl or Fuc residues or both, although structures lacking both

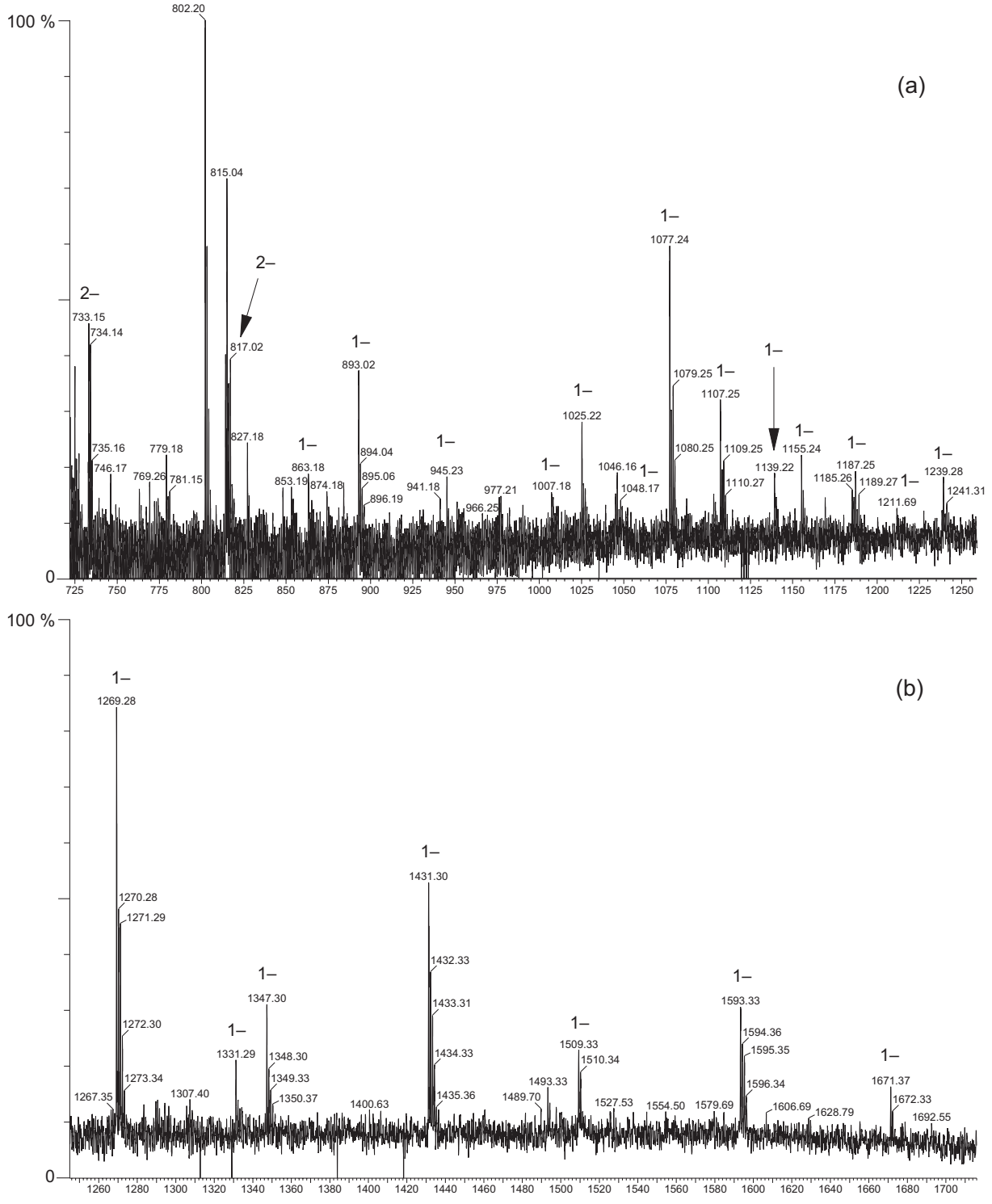


Figure 6. Negative chip-based nanoESI-QTOF MS spectrum of the TW tumour *N*-glycans released with PNGase F from the 42 kDa glycoprotein excised from Coomassie stained gel: assigned structures in the mass range of *m/z* 725–1250 (a) and *m/z* 1250–1700 (b).

Xyl and/or Fuc were also detected. In the shoot sample, however, only a single *N*-glycan structure was observed, which is in good correlation with our previous results. Due to some contaminants in this particular extract, no constant electrospray could be obtained. The highly abundant polysaccharides present in *Mammillaria* plants are viscous in solution and create difficulties in all protein manipulations.[28] Structures, assigned by calculations, originating from the callus and tumour tissue revealed some similarities. In both oligosaccharide mixtures, a high-mannose type *N*-glycan series, $Hex_4HexNAc_2$ – $Hex_7HexNAc_2$, was detected. The second series was assigned by calculations to the complex type *N*-glycans containing pentose and fucose residues ($Hex_2dHex_1HexNAc_2Pent_1$ – $Hex_5dHex_1$-

TABLE III. Assignment of *N*-glycan molecular ions detected by negative chip-based nanoESI-QTOF MS after in-gel release from the 42 kDa TW tumour glycoprotein with PNGase F

| $[M+2Cl]^{2-}$ | $[M+Cl]^-$ | $[M+Na-2H]^-$ | $[M-H]^-$ | Theoretical mass | Proposed structure | *N*-glycan type |
|---|---|---|---|---|---|---|
| | 945.23 | | | 910.33 | $Hex_3HexNAc_2$ | high-mannose |
| | 1107.25 | | | 1072.38 | $Hex_4HexNAc_2$ | high-mannose |
| | 1269.28 | | | 1234.35 | $Hex_5HexNAc_2$ | high-mannose |
| 733.18 | 1431.30 | | | 1396.49 | $Hex_6HexNAc_2$ | high-mannose |
| 814.17 | 1593.33 | | | 1558.54 | $Hex_7HexNAc_2$ | high-mannose |
| | | | 1185.26 | 1186.42 | $Hex_4HexNAc_2Pent_1$-$H_20$ | complex |
| | | | 1347.30 | 1348.41 | $Hex_5HexNAc_2Pent_1$-$H_20$ | complex |
| | | | 1509.33 | 1510.52 | $Hex_6HexNAc_2Pent_1$-$H_20$ | complex |
| | | | 1671.37 | 1672.51 | $Hex_7HexNAc_2Pent_1$-$H_20$ | complex |
| | | | 1007.18 | 1008.37 | $Hex_2dHex_1HexNAc_2Pent_1$-$H_20$ | paucimannosidic |
| | | | 1139.22 | 1140.42 | $Hex_2dHex_1HexNAc_2Pent_2$-$H_20$ | paucimannosidic |
| | | | 1331.29 | 1332.47 | $Hex_4dHex_1HexNAc_2Pent_1$-$H_20$ | complex |
| | | | 1493.33 | 1494.53 | $Hex_5dHex_1HexNAc_2Pent_1$-$H_20$ | complex |
| | | | 1155.24 | 1156.42 | $Hex_3HexNAc_2Pent_2$-$H_20$ | paucimannosidic |
| | 1077.24 | | | 1042.38 | $Hex_3HexNAc_2Pent_1$ | paucimannosidic |
| | 1239.28 | | | 1204.43 | Hex $_4HexNAc_2Pent_1$ | complex |
| | | | 893.02 | 894.32 | $Hex_2dHex_1HexNAc_2$ | paucimannosidic |
| | | | 863.18 | 864.33 | $Hex_1dHex_1HexNAc_2Pent_1$ | paucimannosidic |
| | | 1048.17 | 1025.22 | 1026.38 | $Hex_2dHex_1HexNAc_2Pent_1$ | paucimannosidic |
| | | 1211.69 | 1187.25 | 1188.44 | $Hex_3dHex_1HexNAc_2Pent_1$ | paucimannosidic |

$HexNAc_2Pent_1$). Unusual, probably dehydrated, complex *N*-glycans containing a pentose molecule ($Hex_4HexNAc_2Pent_1$ – $Hex_7HexNAc_2Pent_1$) could be a specific feature in tumour samples. The highest degree of structural heterogeneity was found in the hyperhydric regenerant. It seems that only one single high-mannose structure was present, while the molecular ions were detected in irregular complex type *N*-glycans, among which six structures could contain, by calculations, one or more sialic acid moieties. We probed glycoproteins from four different *Mammillaria* tissues (shoot, callus, hyperhydric regenerants and TW tumour) with biotin- and digoxigenin--labelled lectins from *Sambucus nigra* (SNA I) and *Maackia amurensis* (MAA), revealing terminal sialic acid--(2→6)-α-galactose and sialic acid-(2→3)-α-galactose structures, respectively. Obtained data indicate the presence of sialylated glycoproteins in plant cells. The reason why the same lectins labelled with two different tags were used was the existence of endogenous biotin in various tissues, which can lead to false-positive staining. Since endogenous biotin cannot be differentiated from biotin that is used as a label, all methods that use biotin-countering conjugates are prone to false positive results.[30] After getting the first positive bands with biotin-labelled SNA and MAA, the digoxigenin-labelled lectins were used in order to confirm the obtained results. It was proven that digoxigenin is an excellent label, which in some cases eliminated problems of false positives due to the presence of endogenous biotin.[31] Sialylation was also detected in cultured cells of sugar beet and horse-radish by using the described method with the same lectins,[32] although no signal was observed after the treatment of released *N*-glycans of tobacco microspore and pollen with MAA and SNA.[4] Recent results published by Shah *et al.*[33] developed a discussion about the presence of sialic acids and sialoconjugates in plants. These authors found sialylated glycoconjugates in suspension-cultured cells of *Arabidopsis thaliana* and suggested that there is a genetic and enzymatic basis for sialylation in plants. In contrast, results obtained by Seveno *et al.*[34] do not support the presence of detectable sialic acids in plants. In their opinion, the presence of KDO, an α-ketoacid assumed to be solely found in the cell wall, could lead to misinterpretation of results achieved by reversed-phase C18 chromatography of DMB-sialic acid derivates. In new experiments however, Shah *et al.*[35] observed sialic acid using high pH anion-exchange chromatography with pulsed amperometric

detection that resolved KDO and Neu5Ac residues. Our HPAEC-PAD experiments have demonstrated that Neu5Ac is a constituent of the oligosaccharide chain in 42 kDa glycoproteins from the hyperhydric regenerant and TW tumour. Additionally, by quadrupole time-of-flight electrospray mass spectrometry and accurate mass determination, we could postulate the structure of the following three disialylated species: $Hex_4HexNAc_4NeuAc_2$, $Hex_6HexNAc_4NeuAc_2$, and $Hex_6HexNAc_5NeuAc_2$.

## CONCLUSIONS

It could be deduced from data obtained in this study that the complexity of the N-glycan expression is increasing if the characteristic tissue organization pattern is lost. Hyperhydric shoots regenerated from callus, which morphologically resemble cactus plants but are more round with disarranged spines, are shown to contain a high number and diversity of detected oligosaccharide structures compared to normal shoots. From the callus and TW tumour, however, as two types of unorganized tissues, similar structures of *N*-linked glycans could be postulated, although the glycan mixture from tumour tissue, which has no regeneration potential, revealed structures not present in the callus sample. Novel insights into the correlation of different morphological levels in plant tissues with *N*-glycan composition of the analyzed cellular glycoprotein have been provided in this study, although the here presented glycan pattern data require further detailed analysis by sequencing.

*Acknowledgements.* – Financial support to this work was provided by Deutsche Forschungsgemeinschaft within Sonderforschungsbereich 492, project Z2 to J.P.-K. and by The Ministry of Science and Education of the Republic of Croatia within the project »Proteins and sugars in plant development« to M.K-R. B.B. was supported at the University of Muenster by the Federation of European Biochemical Societies (FEBS) short-term fellowship in 2004.

## REFERENCES

1. P. Lerouge, M. Cabanes-Macheteau, C. Rayon, A. C. Fitchette-Laine, V. Gomord, and L. Faye, *Plant Mol. Biol.* **38** (1998) 31–48.
2. C. Rayon, P. Lerouge, and L. Faye, *J. Exp. Bot.* **49** (1998) 1463–1472.
3. M. Bardor, L. C. Faye, and P. Lerouge, *Trends Plant Sci.* **4** (1999) 376–380.
4. P. Hrubá and J. Tupý, *Plant Sci.* **141** (1999) 29–40.
5. H. Ueda and H. Ogawa, *Trends Glycosci. Glyc*. **11** (1999) 413–428.
6. V. Gomord and L. Faye, *Curr. Opin. Plant Biol.* **7** (2004) 171–181.
7. J. Reinders, U. Lewandrowski, J. Moebius, Y. Wagner, and A. Sickmann, *Proteomics* **4** (2004) 3686–3703.
8. J. Charlwood, J. M. Skehel and P. Camileri, *Anal. Biochem.* **284** (2000) 49–59.
9. P. B. Mills, K. Mills, A. W. Johnson, P. T. Clayton, and B. G. Winchester, *Proteomics* **1** (2001) 778–786.
10. L. H. Stevens, G. M. Stoopen, I. J. W. Elbers, J. W. Molthoff, H. A. C. Bakker, A. Lommen, D. Bosch, and W. Jordi, *Plant Physiol.* **124** (2000) 173–182.
11. I. J. W. Elbers, G. M. Stoopen, H. Bakker, L. H. Stevens, M. Bardor, J. W. Molthoff, W. Jordi, D. Bosch, and A. Lommen, *Plant Physiol.* **126** (2001) 1314–1322.
12. D. Oxley, S. L. Munro, D. J. Craik, and A. Bacic *J. Biochem.* **123** (1998) 978–983.
13. T. Ishimizu, Y. Mitsukami, T. Shinkawa, S. Natsuka, S. Hase, M. Miyagi, F. Sakiyama, and S. Norioka, *Eur. J. Biochem* **263** (1999), 624–634.
14. M. Krsnik-Rasol, H. Čipčić, D. Poljuha, and D. Hagege, *Phyton.* **41** (2000) 13–20.
15. M. A. Elias-Rocha, M. D. Santos-Diaz, and A. Arredondo--Gomez, *Haseltonia* **6** (1998) 96–101.
16. M. Krsnik-Rasol and B. Balen, *Acta Bot. Croat.* **60** (2001) 219–226.
17. T. Murashige and F. Skoog, *Physiol. Plant.* **15** (1962) 473–479.
18. M. M. Bradford, *Anal. Biochem.* **72** (1976) 248–254.
19. U. K. Laemli, *Nature* **227** (1970) 680–685.
20. H. Blum, H. Beier, and H. J. Gross, *Electrophoresis* **8** (1987) 93–99.
21. D. Šagi, J. Peter-Katalinić, H. S. Conradt, and M. Nimtz, *J. Am. Soc. Mass. Spectrom.* **13** (2002) 1138–1148.
22. D. Šagi, C. Schottstädt, K. Lesiewicz, T. Marquardt, and J. Peter-Katalinić, *Proteomics* **5** (2005), 2689–2701.
23. B. Küster, S. Wheeler, A. P. Hunter, R. A. Dwek, and D. J. Harvey, *Anal. Biochem.* **250** (1997) 82–101.
24. A. Zamfir, S. Vakhrushev, A. Sterling, H. Niebel, M. Allen, and J. Peter-Katalinić, *Anal. Chem.* **76** (2004).
25. (http://www.dkfz-heidelberg.de/spec2/sweetdb).
26. A. C. Fitchette-Laine, V. Gomord, A. Chekkafi, and L. Faye, *Plant J.* **5** (1994) 673–682.
27. A. C. Fitchette-Laine, V. Gomord, M. Cabanes, J. C. Michalski, M. Saint Macary, B. Foucher, B. Cavelier, C. Hawes, P. Lerouge, and L. Faye, *Plant J.* **12** (1997) 1411–1417.
28. B. Balen, J. Milošević, and M. Krsnik-Rasol, *Food Technol. Biotechnol.* **40** (2002) 275–280.
29. B. Balen, M. Krsnik-Rasol, I. Zadro, and V. Simeon-Rudolf, *Acta Bot. Croat.* **63** (2004) 83–91.
30. G. Lauc, J. Dumić, S. Šupraha, and M. Flögel, *Food Technol. Biotechnol.* **40** (2002) 363–375.
31. A. Haselbeck, E. Schickaneder, H. von der Eltz, and W. Hosel, *Anal. Biochem.* **191** (1990) 25–30.
32. M. Krsnik-Rasol, D. Pavoković, and P. Peharec, unpublished data.
33. M. M. Shah, K. Fujiyama, C. R. Flynn, and L. Joshi, *Nat. Biotechnol.* **21** (2003) 1470–1471.
34. M. Seveno, M. Bardor, M. Paccalet, V. Gomord, P. Lerouge, and L. Faye, *Nat. Biotechnol.* **22** (2004) 1351–1352.
35. M. M. Shah, K. Fujiyama, C. R. Flynn, and L. Joshi, *Nat. Biotechnol.* **22** (2004) 1352–1353.

## SAŽETAK

### Određivanje *N*-glycana u uzorcima tkiva kaktusa *Mammillaria gracillis* masenom spektrometrijom ESI Q-TOF

**Biljana Balen, Alina Zamfir, Sergey Y. Vakhrushev, Marijana Krsnik-Rasol i Jasna Peter-Katalinić**

*N*-glikani, oslobođeni sa staničnoga glikoproteina od 42 kDa iz izdanka, kalusa, hiperhidriranoga regeneranta i tumora TW uzgojenih u kulturi tkiva kaktusa *Mammillaria gracillis* Pfeiff. analizirani su masenom spektrometrijom nakon deglikozilacije u gelu. Analiza masenom spektrometrijom ESI pokazala je kako su smjese oslobođenih oligosaharida vrlo složene i heterogene, a većina struktura pripadala je kompleksnome tipu *N*-glikana. U uzorku izdanka opažena je samo jedna struktura, što je u skladu s prijašnjim rezultatima. Kalusno i tumorsko tkivo pokazalo je mnogo sličnosti u pripisanim strukturama dok je najveći broj različitih oligosaharida pronađen u hiperhidriranome regenerantu. Na prisutnost sijalinske kiseline ukazala je inkubacija s lektinima, kromatografija ionske izmjene te masena spektrometrija. Rezultati dobiveni u ovim istraživanjima pokazuju da se stupanj organiziranosti tkiva može povezati sa sastavom *N*-glikana staničnih glikoproteina.